

---

# Learning From Context-Agnostic Synthetic Data

---

**Charles Jin**  
CSAIL  
MIT  
Cambridge, MA 02139  
ccj@csail.mit.edu

**Martin Rinard**  
CSAIL  
MIT  
Cambridge, MA 02139  
rinard@csail.mit.edu

## Abstract

We present a new approach for synthesizing training data given only a single example of each class. Rather than learn over a large but fixed dataset of examples, we generate our entire training set using only the synthetic examples provided. The goal is to learn a classifier that generalizes to a non-synthetic domain without pretraining or fine-tuning on any real world data. We evaluate our approach by training neural networks for two standard benchmarks for real-world image classification: on the GTSRB traffic sign recognition benchmark, we achieve 96% test accuracy using only one clean example of each sign on a blank background; on the MNIST handwritten digit benchmark, we achieve 90% test accuracy using a single example of each digit taken from a computer font. Our performance is competitive with state-of-the-art results from the few-shot learning and domain transfer literature, while using significantly less data.

## 1 Introduction

Despite recent advances in deep learning, one central challenge is the large amount of labelled training data required to achieve state-of-the-art performance. Procuring such volumes of high quality, reliably annotated data can be costly or even close to impossible (e.g., obtaining data to train an autonomous navigation system for a lunar probe). Additional hurdles include hidden biases in large datasets [64] and maliciously perturbed (“poisoned”) training data [3, 9, 25, 72].

Synthetic data has seen growing adoption in response to these problems, since the marginal cost of producing new training data is generally very low, and one has full control over the generation process; examples of applications include optical flow [11, 38], segmentation [8, 39], pose estimation [7, 67], face detection [33], visual scene analysis [27], autonomous driving [1, 16, 28, 49, 66, 71], indoor navigation [58], and robotics [32, 63].

However, training with purely synthetic data suffers from the so-called “reality gap”, whereby good performance on synthetic data does not necessarily yield good performance in the real world [26]. One solution is to exploit some small amount of real world data to perform domain adaptation [4]; domain randomization takes this a step further and renders the synthetic domain with *more* variation than real images so that real images appear as just another variation [62].

We propose a new approach to training with synthetic data which focuses solely on the objects of interest and forgoes any information about the context surrounding those objects, where the datasets we use for training consist solely of a single synthetic example per class.

Our contributions are as follows:

1. We formally introduce a decomposition of the input space into object and context spaces, and show how to exploit this decomposition to synthesize data which can efficiently train a classifier that generalizes over a wider domain.

2. We propose an algorithm that leverages this framework to learn visual tasks using context-agnostic synthetic data.
3. We evaluate our approach by training deep neural networks to perform real-world image classification using only a single synthetic example of each class. Compared against methods for domain adaptation and few-shot learning, we achieve state-of-the-art results while using substantially less data.

## 2 Related work

Domain shift, or covariate shift, refers to the problem that occurs when the training set (source domain) and test set (target domain) are drawn from different distributions. In this setting, a classifier which performs well on the source domain may not generalize well in the target domain. A standard method for addressing this challenge is domain adaptation, which leverages some information from the target domain to adapt a function that is learned over the source domain [4]. Algorithms can be either supervised, using small amounts of labelled data [10, 42, 53, 68]; unsupervised, typically requiring large amounts of unlabelled data [2, 14, 17, 23]; or semi-supervised, using a mix [20, 46, 73].

In the context of learning from synthetic data, the domain shift that occurs between synthetic and real world data is known as the reality gap [26]. State-of-the-art rendering engines, such as those used for video games, can help narrow this gap by generating photorealistic data for training [12, 28, 50]. Another technique is using domain randomization to generate the source domain with more variability than is expected in the target domain (e.g., extreme lighting conditions and camera angles), so as to make real images appear as just another variant [62, 66]; in particular, Torres et al. [65] apply domain randomization to traffic sign detection and find that arbitrary natural images suffice for the task. Another body of work exploits generative adversarial networks [21] to generate synthetic domains [24, 36, 56, 61, 69]. Our techniques can be considered a form of domain randomization, except that we compose our backgrounds from the synthetic examples of classes, without any additional data or domain knowledge.

A related approach for learning in the low-data regime is few-shot learning, which aims to learn new classes from a few examples by leveraging prior information. In contrast to domain adaptation, few-shot learning operates under the assumption that the target and source distributions are the same, but the ability to sample certain classes is limited in the source domain. Early approaches emphasized capturing knowledge in a Bayesian framework [13], which was later formulated as Bayesian program learning [34]. Another approach based on metric learning is to find a nonlinear embedding for objects where closeness in the geometry of the embedding generalizes to unseen classes [31, 57, 60, 70]. Few-shot learning via meta-learning aims to extract higher level concepts about learning which can be applied to learn new classes from a few examples [15, 43, 45, 52]. Finally, some works combine domain adaptation with few-shot learning to learn under domain shift and limited samples [41].

The main characteristic that differentiates our work from these approaches is that we operate in the setting where *the entire training set consists solely of a single synthetic image of each class*. In contrast, existing approaches from domain adaptation and few-shot learning only assume that data from the target domain or classes is limited, but still require significant amounts of data from other sources.

## 3 Setting

The standard setting consists of an input space  $\mathcal{X}$ , an output space  $\mathcal{Y}$ , and a hypothesis space  $\mathcal{H}$  of functions mapping  $\mathcal{X}$  to  $\mathcal{Y}$ . We define a domain  $D = (P_D, \mathcal{X}_D)$  to be an input domain  $\mathcal{X}_D \subseteq \mathcal{X}$  along with a probability distribution  $P_D$  with support  $\mathcal{X}_D$ . Without loss of generality, assume that every point  $\mathcal{X}$  has a single universally correct label  $\mathcal{Y}$  which holds regardless of the domain. A loss function is a nonnegative function defined on  $\mathcal{Y} \times \mathcal{Y}$  that measures the difference between two output points. Given a target domain  $D_T$  and a loss function  $\ell$ , the goal is to learn a classifier that minimizes the risk, which is defined as the expected loss  $R_{D_T}(h) := \mathbb{E}_{P_{D_T}}[\ell(h(x), y)]$ . We say that the problem is realizable if there exists some  $h^* \in \mathcal{H}$  such that  $R_{D_T}(h^*) = 0$ .

In supervised learning, we draw  $n$  samples  $(x_1, y_1), \dots, (x_n, y_n)$  from a source domain  $D_S$  and return the classifier which minimizes the empirical risk  $R_{emp}(h) = \frac{1}{n} \sum_i \ell(h(x_i), y_i)$ . If  $D_S$  is a good

approximation for  $D_T$ , given enough samples, a classifier with low empirical risk in the source domain also achieves low risk in the target domain. In practice, this assumption may fail to hold in varying degrees, whether by design, accident, or necessity; however, we would still like to learn a classifier for  $D_T$ . Few-shot learning attempts to overcome the problem where samples for certain classes are scarce in  $D_S$  by combining prior information with a few labelled examples; domain adaptation tries to handle the situation where there is only limited access to  $D_T$  by first training on a more available source domain, then learning a transformation between the source and target domains.

### 3.1 Context agnostic learning

We approach this problem from a different angle. Our new setting consists of an object space  $\mathcal{O}$ , a context space  $\mathcal{C}$ , and an observation function  $\gamma$  with domain  $\mathcal{O} \times \mathcal{C}$ . The input space  $\mathcal{X}$  is then defined as the image of  $\gamma : \mathcal{O} \times \mathcal{C} \rightarrow \mathcal{X} \subseteq \mathcal{C}$ . As before, points in  $\mathcal{O}$  are associated with a single label in  $\mathcal{Y}$ , which induces a label in  $\mathcal{X}$  via  $\gamma$ . We assume that  $\gamma$  is injective in  $\mathcal{O}$  but not necessarily in  $\mathcal{C}$ . Conceptually, the context space is an “ambient space” containing not only valid inputs, but also random noise or irrelevant classes; the input space is thus defined to be the subset of the context space for which there exists a valid label. For example, in our experiments we explore such a decomposition for the task of sign recognition, where the object space  $\mathcal{O}$  consists of traffic signs in all poses, the context space  $\mathcal{C}$  is the (unconstrained) background, and the input space  $\mathcal{X}$  is the set of images which contain a traffic sign.

As before, our objective is to learn a good classifier for an unknown subdomain  $D_T \subseteq \mathcal{X}$ . We consider instead the task of learning a classifier on the entire input space  $\mathcal{X}$ . To sample from  $\mathcal{X}$  we are given oracle access to the observation function and draw (labelled) samples from  $\mathcal{O}$  and  $\mathcal{C}$  independently. Clearly, if this problem is realizable, then we do not even need to know the target domain  $D_T$ , since

$$\mathcal{X}_{D_T} \subseteq \mathcal{X} \implies [R(h^*) = 0 \implies R_{D_T}(h^*) = 0] \quad (1)$$

Then given unlimited sample access to  $\mathcal{X}$  through  $\gamma$ , we can learn  $h^*$  simply by taking the number of samples to infinity. Unfortunately, learning a classifier on  $\mathcal{X}$  generally requires many more samples than learning a classifier on  $\mathcal{X}_{D_T}$ . Thus we aim not just to learn  $h^*$  but rather to learn  $h^*$  using as few samples as possible.

Our goal is therefore to learn an end-to-end classifier directly over  $\mathcal{X}$  which depends only on signals from  $\mathcal{O}$ ; we call this approach *context agnostic learning*. Our hope is to fully capture the lower dimensional structure of  $\mathcal{O}$  in relatively fewer samples. Note, however, that while we only need  $\max(|\mathcal{O}|, |\mathcal{C}|)$  samples to observe every object and context once, we need  $|\mathcal{O}| * |\mathcal{C}|$  samples to observe every object in every context. Hence the main challenge when the number of samples is low will be avoiding *spurious signals*, i.e., statistical correlations between context and objects (and by extension, labels) which are artifacts of the sampling process and do not generalize outside the training set. To avoid relying on random sampling and the law of large numbers, our strategy will be to select samples which actively minimize spurious signals from the context space, so as to force the classifier to depend only on signals from the object space.

### 3.2 Efficient sampling for object-context decomposed input spaces

We develop a formal notion of bias to capture the intuition that reducing spurious signals helps learn a classifier efficiently. To simplify notation, we assume a binary classifier  $h$  which accepts  $o$  and  $c$  as input directly  $h : \mathcal{O} \times \mathcal{C} \rightarrow \{-1, 1\}$ . For an object  $o$ , denote the correct classification  $o^*$ , the expected classification  $\bar{o} := \mathbb{E}_{c \sim \mathcal{C}}[h(o, c)]$ , and the classification error  $\hat{o} := |o^* - \bar{o}|$ . We define the bias  $B(h, c)$  of  $h$  on the context  $c$  to be

$$\begin{aligned} \text{sgn}(B(h, c)) &:= \text{sgn}(\mathbb{E}_{o \sim \mathcal{O}}[h(o, c) - \bar{o}]) \\ \|B(h, c)\| &:= \mathbb{E}_{o \sim \mathcal{O}}[\ell(h(o, c), \bar{o})] \end{aligned}$$

where  $\ell$  is the hinge loss  $\ell(i, j) := \max(0, 1 - i * j)$ . The sign of the bias corresponds to the label toward which the classifier is biased; the magnitude measures the strength of this bias.

The following proposition gives an upper bound on the risk in terms of the bias on  $\mathcal{C}$  and classification error over  $\mathcal{O}$ .

---

**Algorithm 1: Greedy Bias Correction**

---

**Input:** Object space  $\mathcal{O}$ , context space  $\mathcal{C}$ , observation function  $\gamma$ , number of rounds  $R$ , resample probability  $p$ , classifier update subroutine  $\text{Fit}$ , binary classifier  $h$

**Output:** Trained classifier  $h$

```
// initialize random context and label
 $c \sim \mathcal{C}$ ;
 $y \sim \{-1, 1\}$ ;
for  $r \leftarrow 1$  to  $R$  do
   $o \sim \mathcal{O}(y)$ ; // sample object
   $x \leftarrow \gamma(o, c)$ ; // observe object and context
   $h \leftarrow \text{Fit}(h, x, y)$ ; // perform classifier update
  // update context and label
   $p' \leftarrow \text{Uniform}(0, 1)$ ;
  if  $p' < p$  then
    // resample random context and label
     $c \sim \mathcal{C}$ ;
     $y \sim \{-1, 1\}$ ;
  else
     $c \leftarrow x$ ; // previous image becomes new context
     $y \leftarrow -y$ ; // flip label
  end
end
```

---

**Proposition 3.1.** *Let  $h$  be a classifier with average bias  $K$  and classification error for all objects bounded from above by  $\alpha < 1$ . Then the risk is bounded from above by  $K/(2 - \alpha)$ . Furthermore equality holds if and only if all classification errors equal  $\alpha$ .*

We give a proof in Appendix A. The requirement  $\alpha < 1$  ensures the classifier performs better than random guessing. Note that the error bound  $\alpha$  and bias bound  $K$  are not independent; in particular,  $\alpha = 0$  if and only if  $K = 0$  and  $\alpha < 1$ .

The central idea behind Proposition 3.1 is leveraging the fact that labels depend only on objects to factor the risk into separate terms for classification error and bias. This factorization enables us to exploit our ability to sample independently from the object and context spaces. More specifically, we will use samples from  $\mathcal{O}$  to minimize the classification error, and samples from  $\mathcal{C}$  to minimize the bias. Since our operating assumption is that  $\mathcal{O}$  is “easy” to learn, we continue to draw objects randomly; however given an object  $o$ , we aim to observe it with the context for which the classifier has the strongest opposing bias. Intuitively, this allows the classifier to “correct” its bias and unlearn the spurious signals, thereby minimizing the bias and thus the risk.

Adopting this approach without modification requires computing the bias of every context in  $\mathcal{C}$ . In most cases, however, even estimating a single bias may be prohibitively expensive. Thus, rather than solve for the maximum bias explicitly, we instead propose an efficient algorithm which approximately identifies a context with large bias. For the first training sample, given the classifier is initialized without bias, we can just sample the context (and object) uniformly at random and train on the input  $x_1 = \gamma(o_1, c_1), y_1$ . At this point, we observe that a reasonable assumption is that the classifier is biased toward  $y_1$  on the context  $x_1$ ; thus for the next step, we sample  $o_2$  with label  $y_2 = -y_1$  and train on  $x_2 = \gamma(o_2, x_1), y_2$ . More generally, if we adopt the prior that the strongest bias always comes from the most recent training point, we can use a greedy algorithm to correct biases. We call this algorithm Greedy Bias Correction and present a description in Algorithm 1. In addition to the steps detailed above, we also introduce a parameter  $p$  for resetting the context and label back to random so as to ensure proper coverage of the sample spaces.

Note that the algorithm relies crucially on two points: first, the decomposition of the input space into object and context spaces gives us the ability to apply Proposition 3.1 and adaptively observe objects against biased contexts, essentially boosting the signal on objects while correcting biases; second, the abstraction of the input space as a subset of the context space enables us to approximately identify these biased contexts for free.

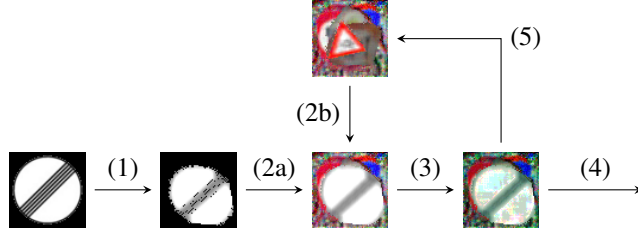


Figure 1: A graphical representation of the generative loop in Algorithm 2 using real training data. (1) Sample from object space. (2) Observe object and context. (3) Perform local refinement. (4) Add to training set. (5) Previous image becomes next context (resample from  $\mathcal{C}$  with probability  $p$ ).

#### 4 Learning visual tasks using context-agnostic synthetic data

We introduce an instantiation of Greedy Bias Correction for learning visual tasks using synthetic data. We are given a function which takes a label  $y$  and outputs a rendering of the corresponding class in a random pose without any background. The context is the background of the object, for which we place no restrictions. The observation function  $\gamma$  simply superimposes an object over a background.

**Local refinement via robustness training** We note that our observation function  $\gamma$  is fairly restrictive; for instance, we do not support occlusions. Because our ultimate goal will be to perform on data taken from a real-world context, we aim to capture this discrepancy using robustness training.<sup>1</sup> In particular, we assume that the image of  $\gamma$  is an  $\epsilon$ -covering of  $\mathcal{X}$ , where a set  $A$  is said to be an  $\epsilon$ -covering of another set  $B$  iff for all points  $b \in B$ , there exists a point  $a$  such that  $\|a - b\| \leq \epsilon$ . Then for a given sample, we will instead add the point in the  $\epsilon$ -neighborhood of  $x$  which maximizes the training loss, i.e., for a classifier  $h$  and a sample  $x = \gamma(o, c)$ , we use  $x' = \operatorname{argmax}_{x' \in N_\epsilon(x)} \ell(h(x'), y)$ . This formulation is often used to train models which are robust against local perturbations. An empirically effective method for finding approximations to  $x'$  is known as Projected Gradient Descent (PGD) [22, 37]. The algorithm can be summarized as

$$x_0 \leftarrow x + \delta$$

$$x_i \leftarrow \Pi_{x+\epsilon}(x_{i-1} + \alpha \cdot \operatorname{sgn}(\nabla_x \ell(h(x_{i-1}), y))), \quad i = 1, \dots, n$$

where  $\delta$  is a small amount of random noise,  $\Pi$  is the projection back onto to the  $\epsilon$ -ball,  $\alpha$  is the step size, and  $n$  is the number of iterations. As is standard for robustness training, we use the  $\ell_\infty$  norm defined as  $\|(x_1, \dots, x_n)\|_\infty = \max_i x_i$ . Our choice of  $\epsilon$  will depend on the task at hand, and we also use different  $\epsilon$  for the portions of the image corresponding to the object and context.

Additionally, since we are no longer in a binary context, we sample a random permutation on labels instead of flipping the label deterministically. The full algorithm is presented as Algorithm 2 in Appendix B; Figure 1 provides a visualization of the key generative process, with images taken from a real step of training a deep neural network to perform classification of traffic signs.

From a practical standpoint, this algorithm makes concrete several benefits of our approach. First, rendering object classes, i.e. sampling from  $\mathcal{O}$ , is often relatively easy. In the case of two-dimensional rigid body objects, this can be captured using standard data augmentation such as rotations, flips, and perspective distortions. Indeed, in this setting, our work can be viewed as a form of minimal one-shot learning, where the input data consists solely of a single unobstructed straight-on shot for each object class. Second, there is no requirement to perform realistic rendering of contexts  $\mathcal{C}$ , avoiding an additional layer of complexity.

Finally, because our approach is context agnostic, our functions are learned without any reference to target domains. In the formal setting, we assumed that the target domain was contained in the image of the observation function; however, synthetic images will always be subject to the reality gap. Our experiments suggest that our approach overcomes this barrier and successfully generalizes to natural images while training on synthetic data only.

<sup>1</sup>Robustness training is more commonly referred to as adversarial training in the adversarial learning community whence we borrow this technique. We use the nonstandard term to avoid confusion with the unrelated (generative) adversarial methods found in the few-shot learning literature.



Figure 2: Images from the training (top) and test (bottom) set for GTSRB (left) and MNIST (right).

## 5 Experiments

We evaluate our approach to learning visual tasks using synthetic data on two common benchmarks for image recognition. Our training sets consist of a single synthetic image for each object class with no additional information about the target domain; Figure 2 shows examples of corresponding classes from the training and test sets of the two benchmarks.

On both benchmarks, our models match previous state-of-the-art results from related settings using few-shot learning and domain adaptation. When multiple experiments are reported for the same approach, we compare against both the most accurate result as well as the result using the least amount of target data. We distinguish between labelled (**L**) and unlabelled (**UL**) data; experiments for which the training data is not known are marked (?).

To isolate the effects of our approach to context agnostic learning, we also report the results of several ablation studies. All strategies employ the same data augmentation (corresponding to sampling from the object space) and use the following techniques for sampling from the context space: **baseline** picks a fresh random background for each training point; **random-context** picks a fresh random background for each batch; **refinement-only** is the same as random-context with the addition of PGD-based refinement; **image-as-context** uses previous training images as contexts; **full** is the full algorithm as described in Algorithm 2. Examples of rendered training data from each approach are shown in Appendix D.

We used PyTorch 1.5.0 [47] and OpenCV 4.2.0 [6] for all experiments; Appendix C provides full setup and training details. Sample images from all datasets, including those used by comparison methods, are shown in Appendix D.

### 5.1 GTSRB

The German Traffic Sign Recognition Benchmark (**GTSRB**) [59] contains 39,209 training and 12,630 test images of 43 classes of German traffic signs taken from the real world. Our training set consists of a single, canonical pictogram of each class taken from the visualization software accompanying the dataset, which we refer to as **Picto**. For data augmentation we used the PyTorch transforms `RandomAffine`, `RandomPerspective`, and `ColorJitter`; OpenCV box blur; and random exposure adjustment. We achieve 95.9% accuracy on the GTSRB test set training only on **Picto**, against a human baseline of 98.8%. Full results are reported in Table 1.

**SynSign** [40] is a synthetic dataset designed to provide realistic training data for traffic sign recognition. The dataset comprises 100,000 synthetically generated images of signs from Sweden, Germany, and Belgium in a variety of poses, rendered against domain-appropriate real-world images (e.g. trees, roads, sky). The dataset contains a superset of the GTSRB classes; as a result, Saito et al. [54] report 79.2% accuracy by training directly on SynSign. In comparison, our baseline using solely data augmentation only achieves 72.0% accuracy, which confirms that training with realistic backgrounds yields an improvement over simple random noise. However, our refinement-only and image-as-context baselines achieve higher accuracy at 86.4% and 87.3%, respectively. Both methods leverage the background of training images to actively combat learning spurious signals, which results in completely unrealistic backgrounds; this suggests that learning context-agnostic features is more effective than using realistic backgrounds.

For domain adaptation, all approaches train on the full 100,000 images in SynSign in addition to some amount of the GTSRB training set. ATT [54] is the only non-baseline method with better performance than ours, achieving 0.3% higher accuracy; however they use 31,367 unlabelled images from the GTSRB training set (in addition to SynSign). Methods using few-shot learning train on roughly half of the data (22 classes) from the GTSRB training set. The leading few-shot learning

Table 1: GTSRB results.

Approach	Method	Training Data		Accuracy (%)
		Source	Target	
Baselines	Source Only (Saito et al. [54])	SynSign		79.2
	Human (Stallkamp et al. [59])			98.8
	Target Only (Ganin et al. [18])		All L	99.8
Few-Shot Learning	VPE (Kim et al. [30]) <sup>§</sup>	Picto*	22 classes L	83.8
	MatchNet (Vinyals et al. [70]) <sup>§</sup>		22 classes L	53.3
	QuadNet (Kim et al. [29]) <sup>§†</sup>		22 classes L	45.3
Domain Adaptation	DSN (Bousmalis et al. [5])	SynSign	1280 UL	93.0
	ML (Schoenauer-Sebag et al. [55]) <sup>§</sup>	SynSign	22 classes L	89.1
	MADA (Pei et al. [48]) <sup>§‡</sup>	SynSign	22 classes L	84.8
	DANN (Ganin et al. [18])	SynSign	31367 UL	88.7
	ATT (Saito et al. [54])	SynSign	31367 UL	<b>96.2</b>
Context Agnostic	baseline	Picto		72.0
	+ random-context	Picto		72.1
	+ refinement-only	Picto		86.4
	+ image-as-context	Picto		87.3
	+ full	Picto		<b>95.9</b>

<sup>§</sup>Test accuracy on remaining 21 unseen classes.

\*Kim et al. [30] use a pictographic dataset similar to Picto.

<sup>†</sup>Reported in Kim et al. [30].

<sup>‡</sup>Reported in Schoenauer-Sebag et al. [55].

approach, VPE [30], adds a pictographic dataset similar to Picto, but achieves only 83.79% accuracy. In comparison, our training set consists of only 43 images, none of which are from GTSRB.

## 5.2 MNIST

**MNIST** [35] consists of 60,000 training and 10,000 test images of handwritten Arabic numerals in grayscale against a blank background. Our training set, **Font**, consists of a single example of each digit taken from a standard digital font. For data augmentation, we use the Pytorch transforms RandomAffine and RandomPerspective; and OpenCV box blur. In order for inputs to have a well-defined ground truth label, we use an observation function which blends the object with the context at a 2:1 ratio. We achieve 90.2% accuracy on the MNIST test set training only on Font, compared to human accuracy of 98%. Table 2 compiles the full results.

MNIST and GTSRB present conceptually opposed challenges for learning: in GTSRB, the classes are rigid two-dimensional objects and backgrounds are complex settings in the natural world; in MNIST, backgrounds are uniform, but classes no longer have a strict specification and individual examples exhibit high variability. Thus, the main challenge of MNIST is learning how to generalize over each object class. Despite the variation in each class, our baseline model trained on Font with plain data augmentation was able to achieve 81.9% accuracy, which exceeds many of the results from domain adaptation and all the approaches using one-shot learning.

The **Omniglot** [34] dataset consists of 1623 hand-written characters from 50 different alphabets, with 20 samples each. Omniglot is often described as an MNIST-transpose, where the goal is learn handwriting rather than specific symbols [31]. Several approaches apply few-shot learning from Omniglot to MNIST, with the idea of transferring extracted features from human handwriting. However the one-shot experiments all perform worse than even our baseline approach. We hypothesize that MNIST may be particularly difficult for one-shot learning since any two examples will likely exhibit high “variance”; conversely, context agnostic learning benefits from using a canonical form which might be closer to the “mean” representation.

Table 2: MNIST results.

Approach	Method	Training Data		Accuracy (%)
		Source	Target	
Baselines	Human (Netzer et al. [44])			98.0
	Target Only (Tzeng et al. [69])		All L	99.2
Few-Shot Learning	FADA (Motiian et al. [41])	SVHN	1 L / class	72.8
	+ more data	SVHN	7 L / class	87.2
	SiamNet (Koch [31])	Omniglot	1 L / class	70.3
	MatchNet (Vinyals et al. [70])	Omniglot	1 L / class	72.0
	APL (Ramalho and Garnelo [51])	Omniglot	1 L / class	61.0
	+ more data	Omniglot	? <sup>‡</sup>	86.0
Domain Adaptation	DSN (Bousmalis et al. [5])	SVHN	1000 UL	82.7
	DRCN (Ghifary et al. [19])	SVHN	?	81.9
	DANN (Ganin et al. [18])	SVHN	?	73.9
	ATT (Saito et al. [54])	SVHN	? L + 1000 UL	86.0
	ADDA (Tzeng et al. [69])	SVHN	60,000 UL	76.0
	CyCADA (Hoffman et al. [24])	SVHN	60,000 UL	<b>90.4</b>
Context Agnostic	baseline	Font		81.9
	+ random-context	Font		88.3
	+ refinement-only	Font		89.7
	+ image-as-context	Font		89.2
	+ full	Font		<b>90.2</b>

<sup>‡</sup>Cumulative accuracy from adapting over the test set.

Street View House Numbers (SVHN) [44] is a dataset of house numbers obtained from Google Street View with 73,257 training and 26,032 test samples. The domain transfer problem faces a similar challenge as Font, namely, handwriting exhibits different characteristics than house numbers fonts. Nevertheless, we note that SVHN contains far more examples of each digit.

Every approach using domain adaptation (including FADA [41], which falls under both categories) trains using the full SVHN dataset of 73,257 training images, with varying amounts of data from MNIST. The only non-baseline approach to exceed our performance is CyCADA [24], which achieves 0.2% better performance by performing domain adaptation using 60,000 unlabelled images from the MNIST training set (in addition to training on SVHN). All approaches using few-shot learning (except FADA) train on 32,460 images from Omniglot and use as few as one image per class from MNIST; the best result achieves accuracy 3% below ours using 70 images from MNIST. In contrast, we use only 10 images, none of which are from MNIST.

## 6 Conclusion

We introduce a novel approach to learning from synthetic data that leverages the separation between objects and contexts to efficiently train a classifier which generalizes to real world data. On two vision-based tasks, our approach outperforms existing algorithms from domain adaptation and few-shot learning, all of which require not only a large dataset for training but also some limited access to the test distribution; conversely, we obtain our results by training on datasets consisting solely of a single synthetic example of each class. Our results suggest that, contrary to the assumption in prior works using synthetic data, bridging the gap between synthetic data and the real world does not require any natural images or even contextual information at all. More broadly, the ability to learn from single synthetic examples of each class also affords fine-grained control over the data used to train our models, allowing us to sidestep issues of data provenance and integrity entirely.



## References

- [1] Hassan Abu Alhaija, Siva Karthik Mustikovela, Lars Mescheder, Andreas Geiger, and Carsten Rother. Augmented reality meets computer vision : Efficient data generation for urban driving scenes, 2017.
- [2] Mahsa Baktashmotlagh, Mehrtash T Harandi, Brian C Lovell, and Mathieu Salzmann. Unsupervised domain adaptation by domain invariant projection. In *Proceedings of the IEEE International Conference on Computer Vision*, pages 769–776, 2013.
- [3] Battista Biggio, Blaine Nelson, and Pavel Laskov. Poisoning attacks against support vector machines, 2012.
- [4] John Blitzer, Ryan McDonald, and Fernando Pereira. Domain adaptation with structural correspondence learning. In *Proceedings of the 2006 conference on empirical methods in natural language processing*, pages 120–128, 2006.
- [5] Konstantinos Bousmalis, George Trigeorgis, Nathan Silberman, Dilip Krishnan, and Dumitru Erhan. Domain separation networks. In *Advances in neural information processing systems*, pages 343–351, 2016.
- [6] G. Bradski. The OpenCV Library. *Dr. Dobb’s Journal of Software Tools*, 2000.
- [7] Berk Calli, Arjun Singh, Aaron Walsman, Siddhartha Srinivasa, Pieter Abbeel, and Aaron M Dollar. The ycb object and model set: Towards common benchmarks for manipulation research. In *2015 international conference on advanced robotics (ICAR)*, pages 510–517. IEEE, 2015.
- [8] Angel X Chang, Thomas Funkhouser, Leonidas Guibas, Pat Hanrahan, Qixing Huang, Zimo Li, Silvio Savarese, Manolis Savva, Shuran Song, Hao Su, et al. Shapenet: An information-rich 3d model repository. *arXiv preprint arXiv:1512.03012*, 2015.
- [9] Xinyun Chen, Chang Liu, Bo Li, Kimberly Lu, and Dawn Song. Targeted backdoor attacks on deep learning systems using data poisoning. *arXiv preprint arXiv:1712.05526*, 2017.
- [10] Jeff Donahue, Yangqing Jia, Oriol Vinyals, Judy Hoffman, Ning Zhang, Eric Tzeng, and Trevor Darrell. Decaf: A deep convolutional activation feature for generic visual recognition. In *International conference on machine learning*, pages 647–655, 2014.
- [11] Alexey Dosovitskiy, Philipp Fischer, Eddy Ilg, Philip Hausser, Caner Hazirbas, Vladimir Golkov, Patrick Van Der Smagt, Daniel Cremers, and Thomas Brox. FlowNet: Learning optical flow with convolutional networks. In *Proceedings of the IEEE international conference on computer vision*, pages 2758–2766, 2015.
- [12] Alexey Dosovitskiy, German Ros, Felipe Codevilla, Antonio Lopez, and Vladlen Koltun. Carla: An open urban driving simulator. *arXiv preprint arXiv:1711.03938*, 2017.
- [13] Li Fe-Fei et al. A bayesian approach to unsupervised one-shot learning of object categories. In *Proceedings Ninth IEEE International Conference on Computer Vision*, pages 1134–1141. IEEE, 2003.
- [14] Basura Fernando, Amaury Habrard, Marc Sebban, and Tinne Tuytelaars. Unsupervised visual domain adaptation using subspace alignment. In *Proceedings of the IEEE international conference on computer vision*, pages 2960–2967, 2013.
- [15] Chelsea Finn, Pieter Abbeel, and Sergey Levine. Model-agnostic meta-learning for fast adaptation of deep networks. In *Proceedings of the 34th International Conference on Machine Learning-Volume 70*, pages 1126–1135. JMLR. org, 2017.
- [16] Adrien Gaidon, Qiao Wang, Yohann Cabon, and Eleonora Vig. Virtual worlds as proxy for multi-object tracking analysis. In *Proceedings of the IEEE conference on computer vision and pattern recognition*, pages 4340–4349, 2016.
- [17] Yaroslav Ganin and Victor Lempitsky. Unsupervised domain adaptation by backpropagation. *arXiv preprint arXiv:1409.7495*, 2014.
- [18] Yaroslav Ganin, Evgeniya Ustinova, Hana Ajakan, Pascal Germain, Hugo Larochelle, François Laviolette, Mario Marchand, and Victor Lempitsky. Domain-adversarial training of neural networks. *The Journal of Machine Learning Research*, 17(1):2096–2030, 2016.
- [19] Muhammad Ghifary, W. Bastiaan Kleijn, Mengjie Zhang, David Balduzzi, and Wen Li. Deep reconstruction-classification networks for unsupervised domain adaptation, 2016.

- [20] Boqing Gong, Yuan Shi, Fei Sha, and Kristen Grauman. Geodesic flow kernel for unsupervised domain adaptation. In *2012 IEEE Conference on Computer Vision and Pattern Recognition*, pages 2066–2073. IEEE, 2012.
- [21] Ian Goodfellow, Jean Pouget-Abadie, Mehdi Mirza, Bing Xu, David Warde-Farley, Sherjil Ozair, Aaron Courville, and Yoshua Bengio. Generative adversarial nets. In *Advances in neural information processing systems*, pages 2672–2680, 2014.
- [22] Ian J Goodfellow, Jonathon Shlens, and Christian Szegedy. Explaining and harnessing adversarial examples. *arXiv preprint arXiv:1412.6572*, 2014.
- [23] Raghuraman Gopalan, Ruonan Li, and Rama Chellappa. Domain adaptation for object recognition: An unsupervised approach. In *2011 international conference on computer vision*, pages 999–1006. IEEE, 2011.
- [24] Judy Hoffman, Eric Tzeng, Taesung Park, Jun-Yan Zhu, Phillip Isola, Kate Saenko, Alexei A Efros, and Trevor Darrell. Cycada: Cycle-consistent adversarial domain adaptation. *arXiv preprint arXiv:1711.03213*, 2017.
- [25] Matthew Jagielski, Alina Oprea, Battista Biggio, Chang Liu, Cristina Nita-Rotaru, and Bo Li. Manipulating machine learning: Poisoning attacks and countermeasures for regression learning. In *2018 IEEE Symposium on Security and Privacy (SP)*, pages 19–35. IEEE, 2018.
- [26] Nick Jakobi, Phil Husbands, and Inman Harvey. Noise and the reality gap: The use of simulation in evolutionary robotics. In *European Conference on Artificial Life*, pages 704–720. Springer, 1995.
- [27] Justin Johnson, Bharath Hariharan, Laurens van der Maaten, Li Fei-Fei, C Lawrence Zitnick, and Ross Girshick. Clevr: A diagnostic dataset for compositional language and elementary visual reasoning. In *Proceedings of the IEEE Conference on Computer Vision and Pattern Recognition*, pages 2901–2910, 2017.
- [28] Matthew Johnson-Roberson, Charles Barto, Rounak Mehta, Sharath Nittur Sridhar, Karl Rosaen, and Ram Vasudevan. Driving in the matrix: Can virtual worlds replace human-generated annotations for real world tasks? *arXiv preprint arXiv:1610.01983*, 2016.
- [29] Junsik Kim, Seokju Lee, Tae-Hyun Oh, and In So Kweon. Co-domain embedding using deep quadruplet networks for unseen traffic sign recognition. In *Thirty-Second AAAI Conference on Artificial Intelligence*, 2018.
- [30] Junsik Kim, Tae-Hyun Oh, Seokju Lee, Fei Pan, and In So Kweon. Variational prototyping-encoder: One-shot learning with prototypical images. In *Proceedings of the IEEE Conference on Computer Vision and Pattern Recognition*, pages 9462–9470, 2019.
- [31] Gregory Koch. Siamese neural networks for one-shot image recognition. 2015.
- [32] Nathan Koenig and Andrew Howard. Design and use paradigms for gazebo, an open-source multi-robot simulator. In *2004 IEEE/RSJ International Conference on Intelligent Robots and Systems (IROS)(IEEE Cat. No. 04CH37566)*, volume 3, pages 2149–2154. IEEE, 2004.
- [33] Adam Kortylewski, Bernhard Egger, Andreas Schneider, Thomas Gerig, Andreas Morel-Forster, and Thomas Vetter. Analyzing and reducing the damage of dataset bias to face recognition with synthetic data. In *Proceedings of the IEEE Conference on Computer Vision and Pattern Recognition Workshops*, pages 0–0, 2019.
- [34] Brenden M Lake, Ruslan Salakhutdinov, and Joshua B Tenenbaum. Human-level concept learning through probabilistic program induction. *Science*, 350(6266):1332–1338, 2015.
- [35] Yann LeCun. The mnist database of handwritten digits. <http://yann.lecun.com/exdb/mnist/>.
- [36] Ming-Yu Liu, Thomas Breuel, and Jan Kautz. Unsupervised image-to-image translation networks. In *Advances in neural information processing systems*, pages 700–708, 2017.
- [37] Aleksander Madry, Aleksandar Makelov, Ludwig Schmidt, Dimitris Tsipras, and Adrian Vladu. Towards deep learning models resistant to adversarial attacks. *arXiv preprint arXiv:1706.06083*, 2017.
- [38] Nikolaus Mayer, Eddy Ilg, Philip Hausser, Philipp Fischer, Daniel Cremers, Alexey Dosovitskiy, and Thomas Brox. A large dataset to train convolutional networks for disparity, optical flow, and scene flow estimation. In *Proceedings of the IEEE Conference on Computer Vision and Pattern Recognition*, pages 4040–4048, 2016.

- [39] John McCormac, Ankur Handa, Stefan Leutenegger, and Andrew J Davison. Scenenet rgb-d: Can 5m synthetic images beat generic imagenet pre-training on indoor segmentation? In *Proceedings of the IEEE International Conference on Computer Vision*, pages 2678–2687, 2017.
- [40] Boris Moiseev, Artem Konev, Alexander Chigorin, and Anton Konushin. Evaluation of traffic sign recognition methods trained on synthetically generated data. In *International Conference on Advanced Concepts for Intelligent Vision Systems*, pages 576–583. Springer, 2013.
- [41] Saeid Motiian, Quinn Jones, Seyed Iranmanesh, and Gianfranco Doretto. Few-shot adversarial domain adaptation. In I. Guyon, U. V. Luxburg, S. Bengio, H. Wallach, R. Fergus, S. Vishwanathan, and R. Garnett, editors, *Advances in Neural Information Processing Systems 30*, pages 6670–6680. Curran Associates, Inc., 2017. URL <http://papers.nips.cc/paper/7244-few-shot-adversarial-domain-adaptation.pdf>.
- [42] Saeid Motiian, Marco Piccirilli, Donald A Adjeroh, and Gianfranco Doretto. Unified deep supervised domain adaptation and generalization. In *Proceedings of the IEEE International Conference on Computer Vision*, pages 5715–5725, 2017.
- [43] Tsensuren Munkhdalai and Hong Yu. Meta networks. In *Proceedings of the 34th International Conference on Machine Learning-Volume 70*, pages 2554–2563. JMLR. org, 2017.
- [44] Yuval Netzer, Tao Wang, Adam Coates, Alessandro Bissacco, Bo Wu, and Andrew Y Ng. Reading digits in natural images with unsupervised feature learning. 2011.
- [45] Alex Nichol, Joshua Achiam, and John Schulman. On first-order meta-learning algorithms. *arXiv preprint arXiv:1803.02999*, 2018.
- [46] Sinno Jialin Pan, Ivor W Tsang, James T Kwok, and Qiang Yang. Domain adaptation via transfer component analysis. *IEEE Transactions on Neural Networks*, 22(2):199–210, 2010.
- [47] Adam Paszke, Sam Gross, Francisco Massa, Adam Lerer, James Bradbury, Gregory Chanan, Trevor Killeen, Zeming Lin, Natalia Gimelshein, Luca Antiga, Alban Desmaison, Andreas Kopf, Edward Yang, Zachary DeVito, Martin Raison, Alykhan Tejani, Sasank Chilamkurthy, Benoit Steiner, Lu Fang, Junjie Bai, and Soumith Chintala. Pytorch: An imperative style, high-performance deep learning library. In *Advances in Neural Information Processing Systems 32*, pages 8024–8035. Curran Associates, Inc., 2019. URL <http://papers.neurips.cc/paper/9015-pytorch-an-imperative-style-high-performance-deep-learning-library.pdf>.
- [48] Zhongyi Pei, Zhangjie Cao, Mingsheng Long, and Jianmin Wang. Multi-adversarial domain adaptation. In *Thirty-Second AAAI Conference on Artificial Intelligence*, 2018.
- [49] Dean A Pomerleau. Alvin: An autonomous land vehicle in a neural network. In *Advances in neural information processing systems*, pages 305–313, 1989.
- [50] Weichao Qiu and Alan Yuille. Unrealcv: Connecting computer vision to unreal engine. In *European Conference on Computer Vision*, pages 909–916. Springer, 2016.
- [51] Tiago Ramalho and Marta Garnelo. Adaptive posterior learning: few-shot learning with a surprise-based memory module, 2019.
- [52] Sachin Ravi and Hugo Larochelle. Optimization as a model for few-shot learning. 2016.
- [53] Kate Saenko, Brian Kulis, Mario Fritz, and Trevor Darrell. Adapting visual category models to new domains. In *European conference on computer vision*, pages 213–226. Springer, 2010.
- [54] Kuniaki Saito, Yoshitaka Ushiku, and Tatsuya Harada. Asymmetric tri-training for unsupervised domain adaptation. In *Proceedings of the 34th International Conference on Machine Learning-Volume 70*, pages 2988–2997. JMLR. org, 2017.
- [55] Alice Schoenauer-Sebag, Louise Heinrich, Marc Schoenauer, Michele Sebag, Lani F. Wu, and Steve J. Altschuler. Multi-domain adversarial learning, 2019.
- [56] Ashish Shrivastava, Tomas Pfister, Oncel Tuzel, Josh Susskind, Wenda Wang, and Russ Webb. Learning from simulated and unsupervised images through adversarial training, 2016.
- [57] Jake Snell, Kevin Swersky, and Richard Zemel. Prototypical networks for few-shot learning. In *Advances in neural information processing systems*, pages 4077–4087, 2017.

- [58] Shuran Song, Fisher Yu, Andy Zeng, Angel X Chang, Manolis Savva, and Thomas Funkhouser. Semantic scene completion from a single depth image. In *Proceedings of the IEEE Conference on Computer Vision and Pattern Recognition*, pages 1746–1754, 2017.
- [59] J. Stallkamp, M. Schlipsing, J. Salmen, and C. Igel. Man vs. computer: Benchmarking machine learning algorithms for traffic sign recognition. *Neural Networks*, (0):–, 2012. ISSN 0893-6080. doi: 10.1016/j.neunet.2012.02.016. URL <http://www.sciencedirect.com/science/article/pii/S0893608012000457>.
- [60] Flood Sung, Yongxin Yang, Li Zhang, Tao Xiang, Philip HS Torr, and Timothy M Hospedales. Learning to compare: Relation network for few-shot learning. In *Proceedings of the IEEE Conference on Computer Vision and Pattern Recognition*, pages 1199–1208, 2018.
- [61] Yaniv Taigman, Adam Polyak, and Lior Wolf. Unsupervised cross-domain image generation. *arXiv preprint arXiv:1611.02200*, 2016.
- [62] Josh Tobin, Rachel Fong, Alex Ray, Jonas Schneider, Wojciech Zaremba, and Pieter Abbeel. Domain randomization for transferring deep neural networks from simulation to the real world. In *2017 IEEE/RSJ international conference on intelligent robots and systems (IROS)*, pages 23–30. IEEE, 2017.
- [63] Emanuel Todorov, Tom Erez, and Yuval Tassa. Mujoco: A physics engine for model-based control. In *2012 IEEE/RSJ International Conference on Intelligent Robots and Systems*, pages 5026–5033. IEEE, 2012.
- [64] Tatiana Tommasi, Novi Patricia, Barbara Caputo, and Tinne Tuytelaars. A deeper look at dataset bias. In *Domain adaptation in computer vision applications*, pages 37–55. Springer, 2017.
- [65] Lucas Tabelini Torres, Thiago M. Paixão, Rodrigo F. Berriel, Alberto F. De Souza, Claudine Badue, Nicu Sebe, and Thiago Oliveira-Santos. Effortless deep training for traffic sign detection using templates and arbitrary natural images, 2019.
- [66] Jonathan Tremblay, Aayush Prakash, David Acuna, Mark Brophy, Varun Jampani, Cem Anil, Thang To, Eric Cameracci, Shaad Boochoon, and Stan Birchfield. Training deep networks with synthetic data: Bridging the reality gap by domain randomization. In *Proceedings of the IEEE Conference on Computer Vision and Pattern Recognition Workshops*, pages 969–977, 2018.
- [67] Jonathan Tremblay, Thang To, Balakumar Sundaralingam, Yu Xiang, Dieter Fox, and Stan Birchfield. Deep object pose estimation for semantic robotic grasping of household objects, 2018.
- [68] Eric Tzeng, Judy Hoffman, Trevor Darrell, and Kate Saenko. Simultaneous deep transfer across domains and tasks. In *Proceedings of the IEEE International Conference on Computer Vision*, pages 4068–4076, 2015.
- [69] Eric Tzeng, Judy Hoffman, Kate Saenko, and Trevor Darrell. Adversarial discriminative domain adaptation. In *Proceedings of the IEEE Conference on Computer Vision and Pattern Recognition*, pages 7167–7176, 2017.
- [70] Oriol Vinyals, Charles Blundell, Timothy Lillicrap, Daan Wierstra, et al. Matching networks for one shot learning. In *Advances in neural information processing systems*, pages 3630–3638, 2016.
- [71] Bichen Wu, Alvin Wan, Xiangyu Yue, and Kurt Keutzer. Squeezeseg: Convolutional neural nets with recurrent crf for real-time road-object segmentation from 3d lidar point cloud. In *2018 IEEE International Conference on Robotics and Automation (ICRA)*, pages 1887–1893. IEEE, 2018.
- [72] Huang Xiao, Battista Biggio, Blaine Nelson, Han Xiao, Claudia Eckert, and Fabio Roli. Support vector machines under adversarial label contamination. *Neurocomputing*, 160:53–62, 2015.
- [73] Ting Yao, Yingwei Pan, Chong-Wah Ngo, Houqiang Li, and Tao Mei. Semi-supervised domain adaptation with subspace learning for visual recognition. In *Proceedings of the IEEE conference on Computer Vision and Pattern Recognition*, pages 2142–2150, 2015.

## A Proofs

*Proof of Proposition 3.1.* By the assumption that  $\alpha < 1$ , we have that for all  $o$ , the signs of the expected classification  $\bar{o}$  and correct classification  $o^*$  match, so that  $\alpha \geq \hat{\alpha} = |o^* - \bar{o}| = 1 - |\bar{o}|$ . Then for all  $o$ ,

$$\begin{aligned}
 \ell(\bar{o}, o^*) &= 1 - \bar{o} * o^* \\
 &= 1 - |\bar{o}| \\
 &= \frac{1 + |\bar{o}|}{1 + |\bar{o}|} (1 - |\bar{o}|) \\
 &= \frac{1 - \bar{o} * \bar{o}}{1 + |\bar{o}|} \\
 &= \frac{\ell(\bar{o}, \bar{o})}{1 + |\bar{o}|} \\
 &\leq \frac{\ell(\bar{o}, \bar{o})}{2 - \alpha}
 \end{aligned}$$

Now to bound the risk, we can write,

$$\begin{aligned}
 R(h) &:= \mathbb{E}_{o \sim \mathcal{O}, c \sim \mathcal{C}}[\ell(h(o, c), o^*)] \\
 &= \frac{1}{|\mathcal{C}||\mathcal{O}|} \sum_c \sum_o \ell(h(o, c), o^*) \\
 &= \frac{1}{|\mathcal{O}|} \sum_o \frac{1}{|\mathcal{C}|} \sum_c (1 - h(o, c) * o^*) \\
 &= \frac{1}{|\mathcal{O}|} \sum_o (1 - \bar{o} * o^*) \\
 &\leq \frac{1}{|\mathcal{O}|} \sum_o \frac{1 - \bar{o} * \bar{o}}{2 - \alpha} \\
 &= \frac{1}{(2 - \alpha)|\mathcal{O}|} \sum_o \frac{1}{|\mathcal{C}|} \sum_c (1 - h(o, c) * \bar{o}) \\
 &= \frac{1}{(2 - \alpha)|\mathcal{C}||\mathcal{O}|} \sum_c \sum_o \ell(h(o, c), \bar{o}) \\
 &= \frac{1}{(2 - \alpha)|\mathcal{C}|} \sum_c \|B(h, c)\| \\
 &= \frac{K}{2 - \alpha}
 \end{aligned}$$

as desired. It also follows that equality holds if and only if  $\alpha = \hat{\alpha}$  for all  $o$ . □

## B Greedy Bias Correction for visual tasks

---

**Algorithm 2:** Visual Learning Using Context-Agnostic Synthetic Data

---

**Input:** Object space  $\mathcal{O}$ , context space  $\mathcal{C}$ , random permutations  $\Pi$ , observation function  $\gamma$ , number of rounds  $R$ , batch size  $B$ , number of classes  $N$ , resample probability  $p$ , classifier update subroutine  $\text{Fit}$ , projected gradient descent subroutine  $\text{PGD}$ , classifier  $h$

**Output:** Trained classifier  $h$

```
for  $r \leftarrow 1$  to  $R$  do
  // initialize empty training batch and random contexts
   $X \leftarrow \emptyset$ ;
  for  $n \leftarrow 1$  to  $N$  do
    |  $c_n \sim \mathcal{C}$ ;
  end
  for  $b \leftarrow 1$  to  $B$  do
    // sample random permutation
     $\pi \sim \Pi(N)$ ;
    // generate new training data
    for  $n \leftarrow 1$  to  $N$  do
      |  $o \sim \mathcal{O}(n)$ ; // sample object for class
      |  $x \leftarrow \gamma(o, c_{\pi(n)})$ ; // observe object and random (permuted) context
      |  $x' \leftarrow \text{PGD}(h, x)$ ; // perform local refinement
      |  $X \leftarrow X \cup \{(x', y)\}$ ; // add to training set
      |  $c_n \leftarrow x'$ ; // previous sample becomes next context
    end
    // resample contexts
    for  $n \leftarrow 1$  to  $N$  do
      |  $p' \leftarrow \text{Uniform}(0, 1)$ ;
      | if  $p' < p$  then
      | |  $c_n \sim \mathcal{C}$ ;
      | end
    end
  end
  // perform classifier update
   $h \leftarrow \text{Fit}(h, X)$ ;
end
```

---

## C Experimental setup

For MNIST, we use the two-layer convolutional neural network from the official PyTorch examples for MNIST, with Dropout regularization replaced with pre-activation BatchNorm. To train with Font, the data augmentation consists of PyTorch transforms RandomAffine(15, translate=(.15, .15), scale=(0.75, 1.05), shear=40), RandomPerspective(0.5, p=1); an OpenCV box blur with a random kernel size between 1 and 6 in the x and y dimensions (independently sampled, so not necessarily square); then set the foreground to all pixels with value greater than 0.2. For refinement, we used step sizes of  $\alpha = 1.6/255$  with 8 iterations and no projection ( $\epsilon = \infty$ ). For the observation function, we blend the object with the context at a 2:1 ratio. We train for 300 epochs using the Adam optimizer (learning rate  $1e-4$ , weight decay  $1e-4$ ), with 5 examples of each class per batch and 20 batches per epoch. We report results for the model that achieves the best performance on the training set, checking every 5 epochs.

For GTSRB, we use a 5-layer convolutional neural network adapted from the official PyTorch tutorials. To train with Picto, the data augmentation consists of PyTorch transforms RandomAffine(5, translate=(.15, .15), scale=(0.65, 1.05), shear=5), RandomPerspective(0.5, p=1); ColorJitter(brightness=.8, contrast=.8, saturation=.8, hue=.05); an OpenCV box blur with a random kernel size between 1 and 6 in the x and y dimensions (independently sampled, so not necessarily square); and a random exposure adjustment by adjusting all pixels by the same random amount between  $-30\%$  and  $50\%$ . For refinement, we used step sizes of  $\alpha = 2/255$  with 8 steps and an epsilon of  $\epsilon = 4/255$  for the foreground only. For the observation function, we superimpose the segmented foreground of the transformed pictographic sign over the context. We train for 300 epochs using the Adam optimizer (learning rate  $1e-4$ , weight decay  $1e-4$ ), with 5 examples of each class per batch and 20 batches per epoch. We report results for the model that achieves the best performance on the training set, checking every 5 epochs.

## D Training and test set visualizations

### D.1 Datasets



Figure 3: From top to bottom: samples from the GTSRB test set, Picto dataset, and SynSign dataset.

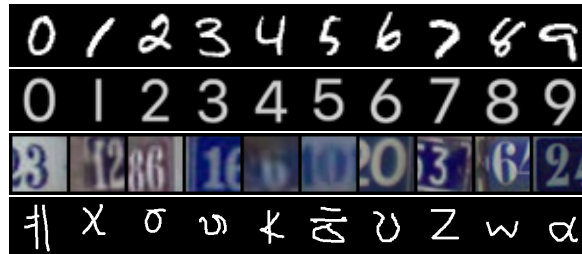


Figure 4: From top to bottom: samples from the MNIST test set, Font dataset, SVHN training set, and Omniglot dataset.



## D.2 Ablation studies



Figure 5: Training images from the ablation studies for the GTSRB benchmark. From top to bottom: baseline, random-context, refinement-only, image-as-context, full.

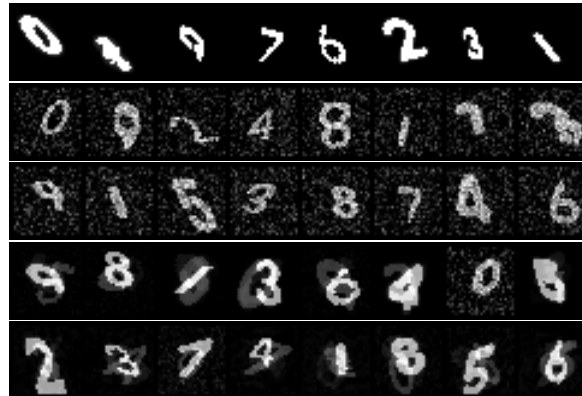


Figure 6: Training images from the ablation studies for the MNIST benchmark. From top to bottom: baseline, random-context, refinement-only, image-as-context, full.